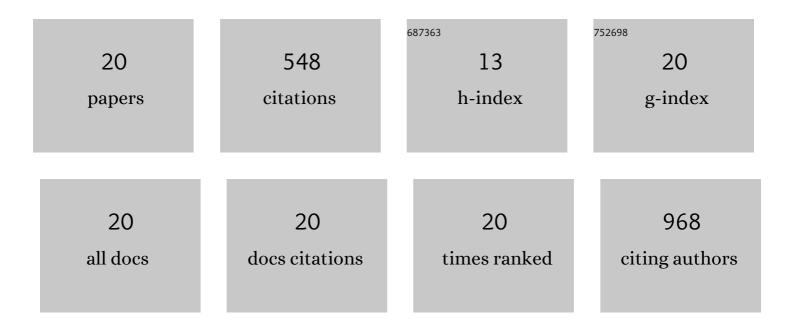
## Sayantani Chall

List of Publications by Year in descending order

Source: https://exaly.com/author-pdf/10915488/publications.pdf Version: 2024-02-01



#	Article	IF	CITATIONS
1	Unveiling the Groove Binding Mechanism of a Biocompatible Naphthalimide-Based Organoselenocyanate with Calf Thymus DNA: An "Ex Vivo―Fluorescence Imaging Application Appended by Biophysical Experiments and Molecular Docking Simulations. Journal of Physical Chemistry B, 2013, 117, 14655-14665.	2.6	113
2	Controlled synthesis of spin glass nickel oxide nanoparticles and evaluation of their potential antimicrobial activity: A cost effective and eco friendly approach. RSC Advances, 2013, 3, 19348.	3.6	96
3	Morphology control of nickel oxalate by soft chemistry and conversion to nickel oxide for application in photocatalysis. RSC Advances, 2013, 3, 6106.	3.6	46
4	Protein Fibril-Templated Biomimetic Synthesis of Highly Fluorescent Gold Nanoclusters and Their Applications in Cysteine Sensing. ACS Omega, 2018, 3, 7703-7714.	3.5	38
5	Tuning the photophysics of a bio-active molecular probe â€~3-pyrazolyl-2-pyrazoline' derivative in different solvents: Dual effect of polarity and hydrogen bonding. Journal of Luminescence, 2010, 130, 2271-2276.	3.1	26
6	Soft-Templated Room Temperature Fabrication of Nanoscale Lanthanum Phosphate: Synthesis, Photoluminescence, and Energy-Transfer Behavior. Journal of Physical Chemistry C, 2013, 117, 25146-25159.	3.1	26
7	An efficient, Schiff-base derivative for selective fluorescence sensing of Zn <sup>2+</sup> ions: quantum chemical calculation appended by real sample application and cell imaging study. Organic and Biomolecular Chemistry, 2014, 12, 6447.	2.8	26
8	Development of a near infrared Au–Ag bimetallic nanocluster for ultrasensitive detection of toxic Pb <sup>2+</sup> ions <i>in vitro</i> and inside cells. Nanoscale Advances, 2019, 1, 3660-3669.	4.6	23
9	Aggregation-Induced Fabrication of Fluorescent Organic Nanorings: Selective Biosensing of Cysteine and Application to Molecular Logic Gate. Langmuir, 2015, 31, 5025-5032.	3.5	21
10	Role of Silver Nanoclusters in the Enhanced Photocatalytic Activity of Cerium Oxide Nanoparticles. European Journal of Inorganic Chemistry, 2018, 2018, 3224-3231.	2.0	20
11	Single step aqueous synthesis of pure rare earth nanoparticles in biocompatible polymer matrices. Journal of Materials Chemistry, 2012, 22, 12538.	6.7	17
12	Spectroscopic and Quantum Mechanical Approach of Solvatochromic Immobilization: Modulation of Electronic Structure and Excited-State Properties of 1,8-Naphthalimide Derivative. Journal of Fluorescence, 2015, 25, 341-353.	2.5	16
13	Nanoparticle Induced Conformational Switch Between α-Helix and β-Sheet Attenuates Immunogenic Response of MPT63. Langmuir, 2018, 34, 8807-8817.	3.5	14
14	Conformational Switch Driven Membrane Pore Formation by <i>Mycobacterium</i> Secretory Protein MPT63 Induces Macrophage Cell Death. ACS Chemical Biology, 2019, 14, 1601-1610.	3.4	14
15	Toxicological assessment of PEG functionalized f-block rare earth phosphate nanorods. Toxicology Research, 2015, 4, 966-975.	2.1	12
16	Polymer-fabricated synthesis of cerium oxide nanoparticles and applications as a green catalyst towards multicomponent transformation with size-dependent activity studies. CrystEngComm, 2016, 18, 7873-7882.	2.6	12
17	Understanding the Effect of Single Cysteine Mutations on Gold Nanoclusters as Studied by Spectroscopy and Density Functional Theory Modeling. Langmuir, 2017, 33, 12120-12129.	3.5	11
18	Micellar charge induced emissive response of a bio-active 3-pyrazolyl-2-pyrazoline derivative: a spectroscopic and quantum chemical analysis. RSC Advances, 2014, 4, 56361-56372.	3.6	7

#	Article	IF	CITATIONS
19	Correlation of FRET efficiency with conformational changes of proteins in ionic and nonionic surfactant environment. Journal of Molecular Liquids, 2016, 213, 33-40.	4.9	6
20	Facile Room Temperature Synthesis of Lanthanum Oxalate Nanorods and Their Interaction with Antioxidative Naphthalimide Derivative. Journal of Nanoscience and Nanotechnology, 2012, 12, 2229-2238.	0.9	4